



# 1 Fungi present distinguishable isotopic signals when grown on 2 glycolytic versus tricarboxylic acid cycle intermediates

3 Stanislav Jabinski<sup>1,2</sup> Vítězslav Kučera<sup>3,4</sup>, Marek Kopáček<sup>1,5</sup>, Jan Jansa<sup>4</sup>, Travis B. Meador<sup>1,2,5\*</sup>  
4

5 <sup>1</sup>University of South Bohemia, Faculty of Science, Department of Ecosystem Biology, Branišovská 1760, 370 05 České  
6 Budějovice, Czechia

7 <sup>2</sup>Institute of Soil Biology and Biochemistry, Biology Centre CAS, Na Sádkách 7, 370 05 České Budějovice, Czechia

8 <sup>3</sup>Charles University, Faculty of Sciences, Albertov 6, 128 00 Praha, Czechia

9 <sup>4</sup>Institute of Microbiology CAS, Vídeňská 1083, 142 20 Praha, Czechia

10 <sup>5</sup>Institute of Hydrobiology, Biology Centre CAS, Na Sádkách 7, 370 05 České Budějovice, Czechia  
11

12 *Correspondence to:* Travis B. Meador (travis.meador@bc.cas.cz)  
13

14 **Abstract.** Microbial activity in soils controls both the size and turnover rates of large carbon (C) inventories stored in the  
15 subsurface, having important consequences for the partitioning of C between terrestrial and atmospheric reservoirs as well as  
16 the recycling of mineral nutrients such as nitrogen or phosphorus (often bound to the C) that support plant growth. Fungi are  
17 major decomposers of soil organic matter (SOM); however, uncertainty in the predominant C substrates that fuel respiration  
18 confound models of fungal production and SOM turnover. To further define the signals of microbial heterotrophic activity, we  
19 applied a dual hydrogen (H) and C stable isotope probing (SIP) approach on pure fungal cultures representing the phyla  
20 Ascomycetes, Basidiomycetes, and Zygomycetes growing on monomeric (glucose, succinate) or complex substrates (tannic  
21 acid,  $\beta$ -cyclodextrin). Our findings demonstrate that the investigated species incorporated only minor amounts of inorganic C  
22 (provided as bicarbonate) into their membrane lipids, amounting to  $< 3\%$  of lipid-C, with no consistent patterns observed  
23 between species or growth substrates. The net incorporation of water-derived H (i.e.,  $\alpha_w$ ) into lipids also did not differ  
24 significantly between incubations with monomeric versus complex substrates; however, growth on succinate solicited  
25 significantly higher  $\alpha_w$  values than glucose or  $\beta$ -cyclodextrin. This finding suggests that <sup>2</sup>H-SIP assays have the potential to  
26 distinguish between microbial communities supported predominantly by substrates that are catabolized by the tricarboxylic  
27 acid cycle versus glycolytic pathway. Furthermore, the average  $\alpha_w$  value of heterotrophic fungal incubations [ $0.69 \pm 0.03$   
28 (SEM)] is consistent with that observed for bacterial heterotrophs, and may be applied for upscaling lipid-based estimates of  
29 fungal production in environmental assays.  
30

## 31 **Short Summary**

32 Microbial production is a key parameter in estimations of organic matter cycling in environmental systems, and fungi play a  
33 major role as decomposers. In order to investigate fungal production and turnover times in soils, we incubated fungal pure  
34 cultures with isotopically labelled water and bicarbonate to investigate growth signals encoded into lipid biomarkers, which  
35 can be applied to improve flux estimates in environmental studies.  
36



## 37 **1 Introduction**

38 Soil organic matter (SOM) is the major reservoir of carbon ( $1580 \times 10^{15}$  g C) in the biosphere, and active microbial populations  
39 act to redistribute this C to other reactive reservoirs, such as atmosphere (Carson et al., 2001; Grinhut et al., 2007). Major  
40 uncertainties in modeling C and climate dynamics stem from insufficient knowledge on the controls of SOM degradation and  
41 transformation (Ciais et al., 2014; Lindahl and Tunlid 2015). Saprotrophic soil fungi are one of the major decomposers in soils,  
42 who are known to degrade naturally occurring complex molecules such as lignin (Kirk & Farrell, 1987; Fioretto et al., 2005;  
43 Baldrian et al., 2011), cellulose (Šnajdr et al., 2011) and humic substances (Grinhut et al., 2007), but are also reported to  
44 compete for accessible plant photosynthate excreted by roots (De Boer et al., 2005; Högberg et al., 2001; Smith & Read, 2008).  
45 Despite the unique and important fungal niche in biogeochemical cycles, their contributions to SOM cycling remains poorly  
46 constrained (Frey 2019; Grinhut et al., 2007). Furthermore, heterotrophic organisms feeding on organic substrates to gain  
47 energy and build biomass are also known to fix a variable amount of inorganic C, in order to replenish intermediates in the  
48 tricarboxylic acid (TCA) cycle (Kornberg 1965). It has been suggested that 2 - 8% of the biomass C in heterotrophs originates  
49 from inorganic C incorporated through anaplerotic carboxylation reactions (Romanenko 1964; Roslev et al., 2004; Braun et  
50 al., 2021). Although, the awareness of these processes has existed for decades (Kornberg 1965; Sorotkin 1966), the relevance  
51 and the metabolic controls on heterotrophic inorganic C fixation remains poorly understood, partly due to the lack of reliable  
52 estimates for most organisms and habitats (Braun et al., 2021).

53 Advanced analytical techniques now allow linking microbial taxa to specific processes in environmental studies by measuring  
54 the incorporation of stable isotopes into biomarkers (Boschker et al., 1998; Dumont and Murrell, 2005; Kreuzer-Martin, 2007),  
55 such as fungal and bacterial membrane lipid fatty acids (Treonis et al., 2004; Willers et al., 2015) or other biomarkers (Boschker  
56 and Middelbourg, 2002). Previous studies have demonstrated that variability in the  $^2\text{H}$  composition of microbial lipids is  
57 redundant with that of environmental water (Hoefs, 2018; Kopf et al., 2015), and stable isotope probing (SIP) assays applying  
58 enrichments in  $^2\text{H}_2\text{O}$  have proven to be a useful tracer of microbial activity in a diverse range of environments (Fischer et al.,  
59 2013; Kellermann et al., 2012; Wegener et al., 2016; Wu et al., 2018). Large H-isotope fractionations, yielding  $\delta^2\text{H}$ -values  
60 between  $-400\%$  and  $+200\%$ , have been observed during biosynthetic incorporation of water hydrogen (water-H) into  
61 individual compounds within a single cell or total biomass, which can be indicative of metabolic processes (Osborn et al.,  
62 2011; Sachse et al., 2012; Zhang et al., 2009). To fully exploit the potential of SIP experiments, a dual-SIP approach was  
63 developed to track total microbial production by adding heavy water ( $^2\text{H}_2\text{O}$ ) together with  $^{13}\text{C}$ -labeled inorganic C (IC),  
64 enabling simultaneous estimates of total and autotrophic metabolism, respectively (Wegener et al., 2012; Wu et al., 2020).  
65 Recently, Jabinski et al. (2024) validated an innovation of the dual-SIP assay by using rapid pyrolysis of fungal biomass to  
66 determine the stable C and H isotopic composition of fungal lipids, and demonstrated that water-H and IC assimilation  
67 signatures could successfully distinguish between fungal ecotypes growing on glucose or glutamic acid as the C source.

68 The aim of the current study was to further assess the controls on water-H and inorganic C incorporation into lipids and expand  
69 our knowledge for interpreting environmental signals by applying the dual-SIP assay on a broader range of pure fungal cultures



70 and growth substrates, including labile monomers versus more complex, high molecular weight molecules. We hypothesized  
71 that I) the incorporation of inorganic C and water-H into the fungal fatty acid biomarker C<sub>18:2</sub> will be similar for fungal species  
72 growing on the same substrate, and II) that inorganic C and water-H incorporation will distinguish between growth on labile  
73 versus more complex C substrates.

## 74 2 Methods

### 75 2.1 Cultivation & Harvesting

76 Fungal pure cultures of two Basidiomycetes (Paxillus involutus (PI, strain SB-22); Phanerodontia chrysosporium (PC, strain  
77 CCM8074)), two Zygomycetes (Mortierella (MO, strain RK-38); Umbelopsis (UM, strain RK-43)) and two Ascomycetes  
78 (*Penicillium jancewskii* (PJ, strain BCCO20\_0265); *Paecilomyces lilacinus* (PL, strain DP-23)) were incubated at 25 °C in the  
79 dark in 500 mL Schott bottles containing 50 mL of a mineral media described previously (Bukovská et al 2018) with the  
80 vitamins left out, which was inoculated with approximately 10<sup>6</sup> spores or a hyphal block < 0.5 cm<sup>3</sup> (Basidiomycetes) recovered  
81 from a previous culture using the same cultivation medium solidified with agar (1.5%).

82 The growth medium contained per liter: 4 g organic C in various forms (C<sub>6</sub>H<sub>12</sub>O<sub>6</sub> glucose; C<sub>4</sub>H<sub>6</sub>O<sub>4</sub> succinic acid; C<sub>42</sub>H<sub>70</sub>O<sub>35</sub> β-  
83 Cyclodextrin or C<sub>76</sub>H<sub>52</sub>O<sub>46</sub> tannic acid), 0.01 g FeSO<sub>4</sub> \* 7H<sub>2</sub>O, 2 g KH<sub>2</sub>PO<sub>4</sub>, 0.5 g MgSO<sub>4</sub> \* 7H<sub>2</sub>O, 0.1 g NaCl, 0.1 g CaCl, 2.5  
84 g (NH<sub>4</sub>)<sub>2</sub>SO<sub>4</sub>, 0.45 g NaHCO<sub>3</sub> and 1 mL of a mixed solution (per liter: 0.5 g H<sub>3</sub>BO<sub>3</sub>, 0.04 g CuSO<sub>4</sub> \* 5H<sub>2</sub>O, 0.1 g KI, 0.4 g  
85 MnSO<sub>4</sub> \* 5H<sub>2</sub>O, 0.2 g NaMoO<sub>4</sub> \* 2H<sub>2</sub>O, 0.4 g ZnSO<sub>4</sub> \* 7H<sub>2</sub>O). The pH of the medium was adjusted to 4.5 before inoculation.  
86 Dual-SIP experiments were performed using <sup>13</sup>C-bicarbonate (<sup>13</sup>C-DIC, NaH<sup>13</sup>CO<sub>3</sub>) and deuterated water (D<sub>2</sub>O). Each fungal  
87 strain was grown in triplicate with non-labeled substrates (Treatment I), with δ<sup>2</sup>H of the medium water adjusted to 100‰ and  
88 10‰ of <sup>13</sup>C-DIC (Treatment II), 200‰ δ<sup>2</sup>H and 10‰ <sup>13</sup>C -DIC (Treatment III), and 400‰ δ<sup>2</sup>H and 10‰ <sup>13</sup>C -DIC (Treatment  
89 IV). The Schott bottles were closed with a rubber stopper in order to keep the labeled <sup>13</sup>C-DIC from outgassing, and ample  
90 headspace was provided to maintain oxic conditions throughout the growth experiment. Fungal growth was monitored via the  
91 accumulation of CO<sub>2</sub> in the headspace, and we aimed to harvest when CO<sub>2</sub> levels reached 10%; however, without preliminary  
92 knowledge of the fungal growth dynamics, some cultivations exceeded this level more quickly than they could be sampled and  
93 analyzed.

94 Mycelia were separated from the growth medium via filtration through 5 μm Isopore polycarbonate filters (47 mm diam, Merck  
95 catalogue number TMTP04700) using vacuum filtration device allowing to collect the cultivation medium into sterile 50 mL  
96 tube. Thereafter, the mycelium was washed with ample MilliQ water, transferred to pre-weighed, sterile 50 mL tubes, fresh  
97 weight of the biomass was recorded, and the samples were frozen at -80 °C until lyophilization. A subsample of the cultivation  
98 medium was also frozen at -80 °C and the rest used to determine pH post-incubation. After lyophilization, the dry weight of  
99 each sample was determined and stored at -20 °C until further analysis.



## 100 2.2 Measurements

### 101 2.2.1 Headspace CO<sub>2</sub> concentration and isotope composition

102 Samples of headspace (0.3 mL) were collected weekly from each bottle into helium flushed 12 mL exetainer vials (Exetainer,  
103 Labco Limited, UK) and analyzed for their CO<sub>2</sub> concentration and <sup>13</sup>C/<sup>12</sup>C isotopic ratio using Gasbench II equipped with a  
104 single cryo-trap connected to Delta V Advantage isotopic ratio mass spectrometer (IRMS) via Conflow IV (Thermo Scientific,  
105 Bremen, Germany). Ambient air (with the CO<sub>2</sub> concentration measured using LiCor 850 gas analyzer previously) was used  
106 as standard for CO<sub>2</sub> concentration measurements, whereas laboratory cylinder with CO<sub>2</sub> gas ( $\delta^{13}\text{C} = -2.86\text{‰}$ ) was used as a  
107 standard for the isotopic composition of the C. The analytical error was below 1‰. Data were analyzed and exported using  
108 the Isodat 3.0 software.

### 109 2.2.2 Medium water (<sup>2</sup>H<sub>2</sub>O)

110 Liquid samples were transferred into 1.5 ml glass vials (32 x 11.6 mm, Fischer Scientific) and then measured using Triple  
111 Liquid Water Isotope Analyzer (Los Gatos Research), which is based on the principle of high-resolution laser absorption  
112 spectroscopy. Samples were dispensed into the instrument using an autosampler (PAL3 LSI, ABB company) and a 1.2  $\mu\text{L}$   
113 syringe (Hamilton). Samples were measured and evaluated against prepared laboratory standards of known isotopic  
114 composition. The isotopic ratios of these laboratory standards were verified by measuring against international standards  
115 (VSMOW2, SLAP2) made by the IAEA. For quality control purposes, the measurements of the samples were also interspersed  
116 with periodic measurements of the prepared verification samples with known isotopic composition. The final isotopic  
117 composition ( $\delta^2\text{H}$ ) was determined using LIMS software. Analytical error of  $\delta^2\text{H}$  was <1.5‰.

118 Water sampled from incubations with tannic acid could not be measured using the laser, as described above, due to its high  
119 organic carbon content, and was rather measured via a GasBench II system (Thermo Scientific, Bremen, Germany; Application  
120 Note: 30049). Medium water samples (200  $\mu\text{L}$ ) were added with a platinum catalyst to a 12 mL exetainer vials (Exetainer,  
121 Labco Limited, UK). The headspace was flushed with 1% H<sub>2</sub> in He at approximately 100 mL min<sup>-1</sup> with for 6 min. After an  
122 equilibration time of over 40 min, the samples were measured by purging the exetainer using a double-holed needle with  
123 helium into a 250  $\mu\text{L}$  sample loop. The sample was then injected and separated via a Carboxen PLOT 1010 (0.53 mm ID;  
124 Supelco, Bellefonte, USA) held at 90 °C with a flow rate of 0.75 bar, and then introduced into the MAT253 Plus IRMS via a  
125 Conflo IV interface. Each sample was injected three times during one analysis. The isotopic composition was determined using  
126 Isodat 3.0 software against the corresponding H<sub>2</sub> working gas (-239‰ for  $\delta^2\text{H}$ ) and the values were corrected and normalized  
127 using international standards VSMOW2 (0‰ for  $\delta^2\text{H}$ ), SLAP2 (-427.5‰ for  $\delta^2\text{H}$ ), USGS53 (+40.2‰ for  $\delta^2\text{H}$ ) and GFLES-2  
128 (159.9‰ for  $\delta^2\text{H}$ ). The analytical error was around 1‰.

129



### 130 **2.2.3 Carbon ( $\delta^{13}\text{C}$ ) substrate analysis**

131 Substrates (~100  $\mu\text{g}$ ) were weighed into tin capsules (8 \* 5 mm, Sercon, Crewe, UK) and placed in a helium-flushed carousel  
132 autosampler, then introduced to an Elemental Analyzer IsoLink device (EA IsoLink CNSOH, Thermo Scientific, Bremen,  
133 Germany) equipped with a CHN/NC/N EA combustion/reduction reactor (Sercon, Crewe, UK) heated to 1020 °C. A pulse of  
134 oxygen was introduced to the reactor simultaneously with the sample. The sample gases were quantified via a thermal  
135 conductivity detector (TCD) and then introduced to a MAT 253 Plus isotope ratio mass spectrometer (IRMS; Thermo  
136 Scientific; Bremen, Germany) via the open split of a Conflo IV interface, with helium as the carrier gas. The isotopic  
137 composition was determined using Isodat 3.0 software against the corresponding CO<sub>2</sub> working gas (-4.191‰ for  $\delta^{13}\text{C}$ ), and  
138 the values were corrected for linearity and normalized to the VPDB scale using international reference material IAEA-600 (-  
139 27.771‰ for  $\delta^{13}\text{C}$ ). The analytical error was <0.04‰.

### 140 **2.2.3 Pyrolysis GC for lipid analysis**

141 The pyrolysis unit Shimadzu 3030D (Shimadzu, Kyoto, Japan/ Frontier Laboratories, Fukushima, Japan) was installed on top  
142 of the GC Trace1310 gas chromatograph SSL injector (Thermo Scientific, Bremen, Germany) and the GC was equipped with  
143 an SLB-IL60 column (non-bonded; 1,12-Di(tripropylphosphonium)dodecane bis(trifluoromethanesulfonyl)imide phase, 30 m,  
144 0.25 mm ID, 0.20  $\mu\text{m}$  df, Supelco, Bellefonte, USA). The furnace temperature was 650 °C and the interface temperature was  
145 370 °C. The injector temperature was 360 °C and the GC oven was held at 80 °C for 1 min then ramped to 175 °C at 15 °C  
146  $\text{min}^{-1}$ , then ramped to 195 °C at 2 °C  $\text{min}^{-1}$ , then ramped to 300 °C at 10 °C  $\text{min}^{-1}$ , and finally held at 300 °C for 7 min. Helium  
147 was used as carrier gas with a constant flow of 1.5 mL  $\text{min}^{-1}$  with a split ratio of 40 and a split flow of 26.7 mL  $\text{min}^{-1}$ . The  
148 column flow was split via a multichannel device to acquire MS and isotopic data simultaneously from one injection. The GC-  
149 MS (ISQ QD; Thermo Scientific, Bremen, Germany) ion source was set to electron impact ionization mode (EI) at 70 eV and  
150 a scan range of m/z 50 – 500 with a scan time of 0.2  $\text{sec}^{-1}$  was applied. Scan started after 8 min to avoid the solvent peak in  
151 the MS. Transfer line temperature was set to 300 °C and the Ion source was set to 250 °C.

152 The samples (freeze-dry biomass, 0.1 mg – 1.3 mg) were weighed into an ultra clean stainless steel Eco-Cup LF (Frontier  
153 Laboratories, Fukushima, Japan) which were burned with a torch before usage to ensure no contamination. FAMES signals  
154 were acquired in the same run. Immediately prior to the measurement, 30  $\mu\text{L}$  of trimethylsulfonium hydroxide (TMSH) was  
155 added to the sample to increase the volatilization of the fatty acids and improve measurement sensitivity. Identification was  
156 performed using fragmentation patterns and the NIST 14 library.

157 Stable carbon and hydrogen isotope compositions of FAMES were determined by splitting the flow from the GC column to a  
158 GC-Isolink II reactor, coupled to a MAT253 Plus IRMS via a Conflo IV interface. Values are expressed in standard delta  
159 notation ( $\delta^{13}\text{C}$  and  $\delta^2\text{H}$ ). MS information was simultaneously acquired by use of the multi-channel device described above.  
160 For conversion of FAMES and ergosterol to CO<sub>2</sub>, the combustion reactor (nickel oxide tube with CuO, NiO, and Pt wires) was  
161 set to 1000 °C. For conversion of FAMES and ergosterol to H<sub>2</sub>, the pyrolysis reactor (aluminum tube) was set to 1420 °C.

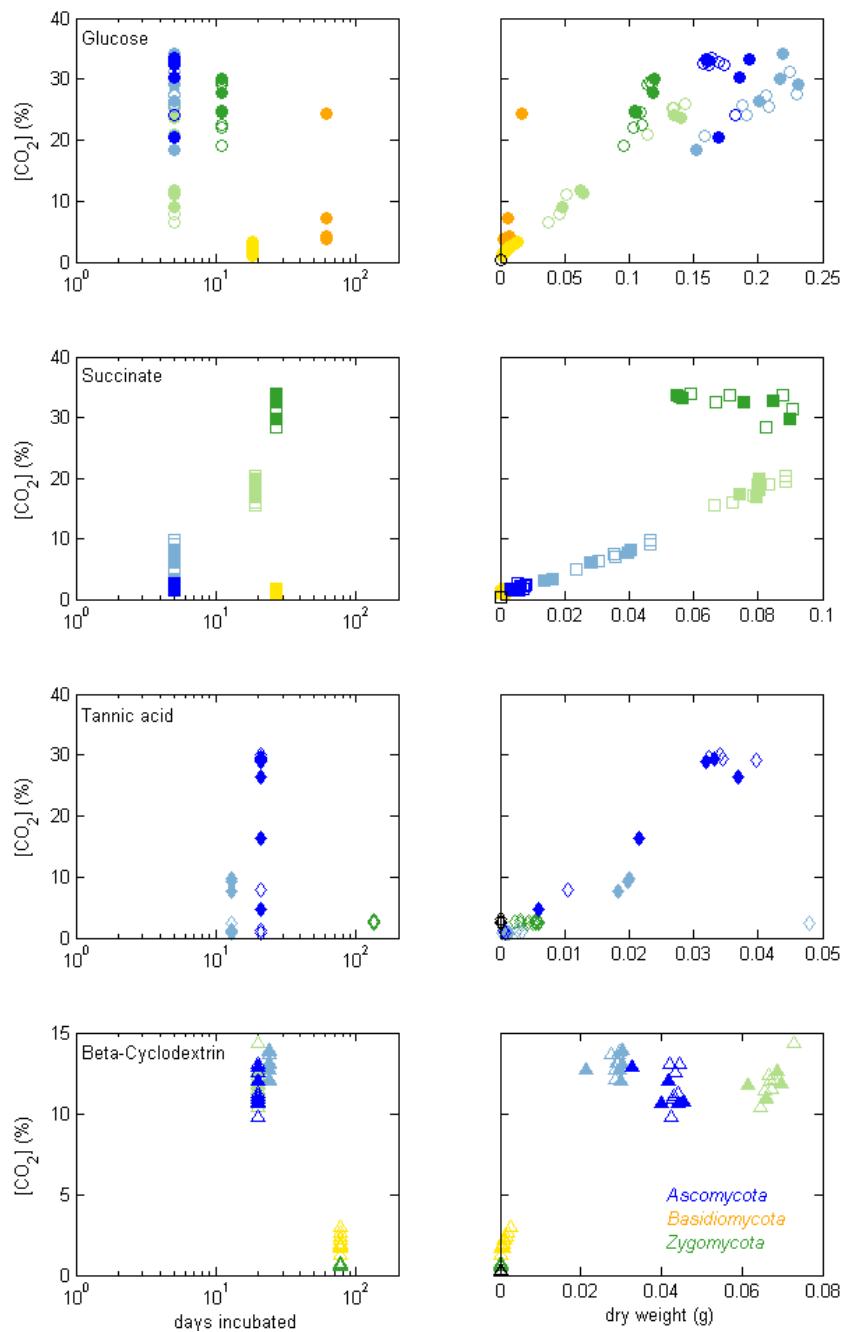


162 FAMEs were identified by their retention times and fragmentation patterns. The isotopic composition was determined using  
163 Isodat 3.0 software against the corresponding CO<sub>2</sub> or H<sub>2</sub> working gas (-4.191‰ for δ<sup>13</sup>C, -239.5‰ for δ<sup>2</sup>H). Isotope corrections  
164 for instrument drifts, linearity, and normalization to the VPDB or VSMOW scales were performed according to the response  
165 of USGS70 (-30.53‰ for δ<sup>13</sup>C, -183.9‰ for δ<sup>2</sup>H) and USGS72 (-1.54‰ for δ<sup>13</sup>C, 348.3‰ for δ<sup>2</sup>H) reference standards. The  
166 analytical error was <0.5‰ and <10‰ for δ<sup>13</sup>C and δ<sup>2</sup>H, respectively.

## 167 **3 Results**

### 168 **3.1 Fungal growth and CO<sub>2</sub> production**

169 All fungal species were pure cultures, which were incubated in a mineral medium with either glucose, succinate, β-  
170 cyclodextrin, or tannic acid serving as the sole organic C source. Growth was monitored by the evolution of CO<sub>2</sub> into the  
171 headspace, which ranged from 0.36% (no respiration of substrate) to a maximum of 35%, after incubation times ranging from  
172 5 to 160 days (Fig. 1). The pH of the media in all incubations ranged from 2 to 5.5 at the time of harvest, with a general trend  
173 of decreasing pH with increasing CO<sub>2</sub>; however, the trend was opposite when succinate was the carbon source, with pH  
174 increasing from 4 to 5.5. For samples that produced sufficient biomass, the dry biomass of harvested fungal hyphae ranged up  
175 to 250 mg, and at least 30 μg dry biomass was used to analyze fungal membrane fatty acids by Pyr-GC-IRMS. Only the  
176 Ascomycetes species PL and PJ grew sufficiently on each tested substrate to produce enough biomass for stable isotope  
177 analysis. Incubations of Zygomycetes species with glucose or succinate also yielded sufficient dry biomass, and only UM and  
178 not MO was able to grow on β-cyclodextrin; Zygomycetes species produced neither CO<sub>2</sub> nor biomass when incubated with  
179 tannic acid. The Basidiomycetes typically exhibited the slowest growth, and both species (PI and PC) only produced enough  
180 biomass when grown on glucose. The CO<sub>2</sub> levels in Basidiomycetes incubations with succinate increased to a maximum of ~  
181 2%, but only PI yielded sufficient biomass for analysis. PC grew sufficiently on β-cyclodextrin, with CO<sub>2</sub> levels increasing to  
182 a maximum of 3%, while CO<sub>2</sub> remained < 0.6% in PI incubations.



183

184 **Figure 1. Growth of fungal species on each substrate as indicated by production of CO<sub>2</sub> versus days of incubation (left panels) or**  
185 **dry biomass (right panels). Filled symbols indicate samples for which the C<sub>18:2</sub> biomarker was measured by Pyr-GC-IRMS. Colors**  
186 **represent the Ascomycetes species PJ (dark blue) and PL (light blue), Zygomycetes species MO (dark green) and UM (light green),**  
187 **and Basidiomycetes species PC (orange) and PI (yellow). The symbols denote incubations with glucose (circles), succinate (squares),**  
188 **tannic acid (diamonds), or β-cyclodextrin (triangles).**

189



190 Fungal respiration of the growth substrates led to decreasing  $\delta^{13}\text{C}$ -CO<sub>2</sub> values as fungal biomass was produced, which followed  
191 a hyperbolic trend expected for the mixing of CO<sub>2</sub> from two different sources (Text S1; c.f., Kendall and Caldwell, 1998). The  
192 atom % <sup>13</sup>C in control incubations with no fungal inoculum was measured at the latest time of harvest of inoculated incubations  
193 and stayed below 0.4% except tannic acid which ranged from 2-3%; the  $\delta^{13}\text{C}$  values of the substrates were glucose = -26.5‰;  
194 succinate = -28.3‰, tannic acid = -27.4‰,  $\beta$ -cyclodextrin = -10.6‰. The mixing relationship was modeled using all CO<sub>2</sub> data,  
195 across all incubations, and integrated to approximate the mixing-weighted average F<sup>13</sup>C value of inorganic C for each  
196 incubation (cf., Text S1, Fig. S2), which was finally applied in the denominator of Eq. 1 to estimate the fraction of lipid-C  
197 derived from inorganic C. For incubations that produced sufficient fungal biomass for stable C isotopic analysis, the weighted  
198 average  $\delta^{13}\text{C}$  values of inorganic C that were applied in Eq. 1 ranged from 200 to 1400 ‰ (i.e., ~ 1.3 to 2.6 AT% <sup>13</sup>C).

## 199 3.2 Stable isotopic composition of fungal lipids

### 200 3.2.1 Carbon isotopes

201 The  $\delta^{13}\text{C}$  values of fungal biomarker C<sub>18:2</sub> was determined as described in section 2.2.4 and is reported in this section as standard  
202 delta values (‰). The inorganic C incorporation into the biomarker was calculated based on the following equation:

$$203 \%IC_{(assimilation)} = \frac{F^{13C}_{lipids\ labeling} - F^{13C}_{lipids\ control}}{F^{13C}_{DIC(medium)} - F^{13C}_{substrate}} \times 100\% \quad (\text{Eq. 1})$$

204 **Equation 1: Inorganic carbon (IC) assimilation was calculated as the difference in the <sup>13</sup>C atom fraction (F<sup>13</sup>C) of the lipids from the**  
205 **labeling experiment compared to the natural (control), relative to the difference between the mixing-weighted average F<sup>13</sup>C of**  
206 **dissolved inorganic C (DIC, cf. Text S1) and the F<sup>13</sup>C of the substrate. F was calculated as F<sup>13</sup>C = (R<sup>13C/12C</sup>)/(R<sup>13C/12C</sup> + 1), where R is**  
207 **calculated from the  $\delta^{13}\text{C}$  ratios as measured with the IRMS equipment using the reverse of the  $\delta$  notations ( $\delta^{13}\text{C} =$**   
208 **( $[\text{<sup>13}\text{C}/\text{<sup>12}\text{C}]_{\text{sample}}/[\text{<sup>13}\text{C}/\text{<sup>12}\text{C}]_{\text{ref}} - 1</sup></sup></sup></sup>$ ) \* 1000 (modified after Boschker & Middelburg 2002; Wegener et al., 2012).**

209 The  $\delta^{13}\text{C}$  values of fungal biomarkers C<sub>18:2</sub> (Table 1) produced under natural cultivation conditions with glucose (i.e., non-  
210 labeled; AT%<sub>DIC</sub> ~ 1%) ranged from -24.1‰ to -21.2‰ across all strains (n = 6 species). As expected, C<sub>18:2</sub> harvested from  
211 the labeled incubations exhibited slightly higher  $\delta^{13}\text{C}$  values (up to +11‰; PC grown on glucose) than the corresponding  
212 experiment amended with natural bicarbonate, likely owing to the incorporation of labeled inorganic C into the C<sub>18:2</sub> fatty acid.

213





214 **Table 1:**  $\delta^{13}\text{C}$  values of fungal biomarker  $\text{C}_{18:2}$  harvested from incubations with non-labeled substrates (nat) or those amended with  
 215  $^{13}\text{C}$ -labeled bicarbonate. Incorporation of inorganic C (%IC) was calculated based on Eq.1. Not all fungal species grew on all  
 216 substrates, and some did not give enough biomass for analysis (n.d\*) and therefore no inorganic C incorporation was calculated  
 217 (n.d). Errors represent the standard deviation of replicate incubations.

<i>Species</i>	Glucose		IC (%)	Succinate		IC (%)	Tannic acid		IC (%)	$\beta$ -cyclodextrin		IC (%)
	$\delta^{13}\text{C}$ (‰)			$\delta^{13}\text{C}$ (‰)			$\delta^{13}\text{C}$ (‰)			$\delta^{13}\text{C}$ (‰)		
	nat	+		nat	+		nat	+		nat	+	
<i>Paxillus involutus (PI)</i>	-21.5	-16.7	0.6 ( $\pm 0.2$ )	n.d*	n.d*	n.d	n.d*	n.d*	n.d	n.d*	n.d*	n.d
<i>Phanerochaete chrysosporium (PC)</i>	-24.1	-15.9	0.9 ( $\pm 0.3$ )	-27.3	-23.5	0.3 ( $\pm 0.1$ )	n.d*	n.d*	n.d	n.d*	n.d*	n.d
<i>Mortierella (MO)</i>	-21.9	-20.7	0.5 ( $\pm 0.1$ )	-31.7	-31.5	0.1 ( $\pm 0.1$ )	n.d*	n.d*	n.d	n.d*	n.d*	n.d
<i>Umbelopsis (UM)</i>	-21.2	-21.1	0.1 ( $\pm 0.0$ )	-30.6	-28.2	0.7 ( $\pm 0.2$ )	n.d*	n.d*	n.d	-21.7	-18.1	0.8 ( $\pm 0.3$ )
<i>Penicillium jancewskii (PJ)</i>	-23.2	-22.1	0.5 ( $\pm 0.2$ )	-30.1	-27.8	0.2 ( $\pm 0.0$ )	-25.9	-20.5	2.2 ( $\pm 0.5$ )	-20.7	-20.1	0.1 ( $\pm 0.2$ )
<i>Paecilomyces lilacinus (PL)</i>	-23.0	-23.5	n.d	-30.8	-29.9	0.1 ( $\pm 0.0$ )	-25.4	-25.0	0.1 ( $\pm 0.0$ )	-19.1	-17.6	0.7 ( $\pm 0.4$ )

218

219 The estimated incorporation of IC into  $\text{C}_{18:2}$  (%IC) typically ranged up to 1%; only PJ grown on tannic acid exhibited higher  
 220 %IC values, which ranged up to 2.2% (Fig. 2). There were no general trends observed in %IC with other measured or estimated  
 221 parameters, including CUE; however, for the two species that were able to grow on tannic acid, %IC was positively correlated  
 222 with the amount of  $\text{CO}_2$  and biomass produced during the incubation ( $R^2 > 0.85$ ,  $n = 5$ ,  $p < 0.01$ ).

223

224

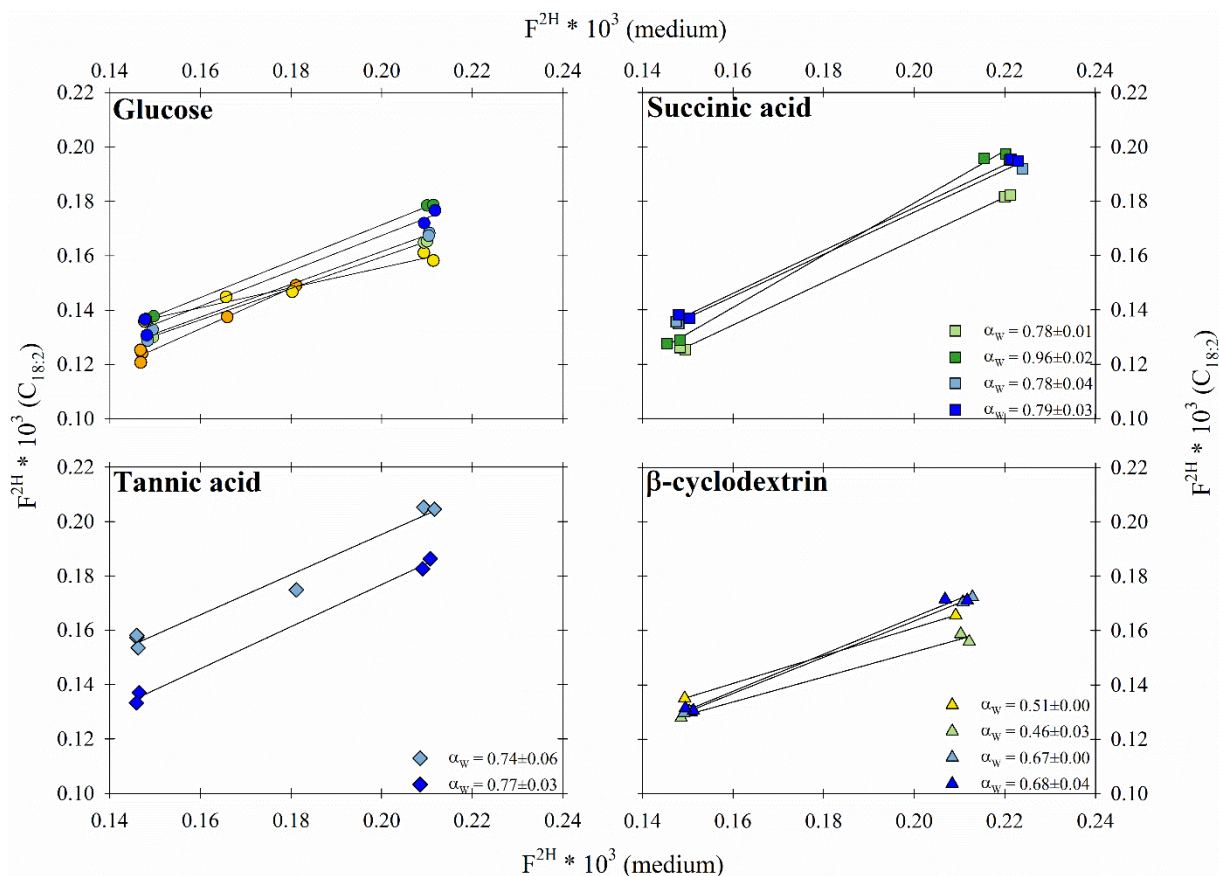
225

226

227

228





243

244 **Figure 3.** The water hydrogen assimilation factor ( $\alpha_w$  values) estimated as the slope of the fractional  $^2\text{H}$  abundance ( $F^{2\text{H}}$ ) in lipids  
245 (y-axis) versus medium water (x-axis). Data are shown for fungal biomarker  $\text{C}_{18:2}$  produced during growth on the different substrates  
246 (glucose, succinic acid, tannic acid and  $\beta$ -cyclodextrin) and harvested from the different fungal species [*Paxillus involutus* (PI),  
247 *Phanerochaete chrysosporium* (PC), *Mortierella* (MO), *Umbelopsis* (UM), *Penicillium jancewskii* (PJ) and *Paecilomyces lilacinus* (PL)].  
248  $R^2$  values for all slopes were  $> 0.97$ .

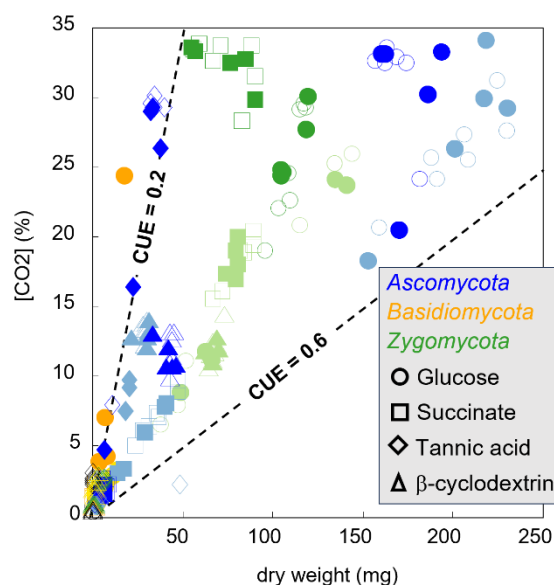
## 249 4 Discussion

### 250 4.1 Fungal growth dynamics

251 Collectively, the fungal incubation experiments included a total of six species representing three different phyla, and exhibited  
252 a large range in the relative amounts of  $\text{CO}_2$  and biomass produced, with the estimated carbon use efficiency [CUE = biomass-  
253  $\text{C} / (\text{CO}_2 + \text{biomass-C})$ ] ranging from 0.2 to 0.6 (Fig. 4). The incubations were initiated under atmospheric, oxic conditions,  
254 such that fungi were able to respire the substrate aerobically. While oxic conditions likely prevailed during most of the  
255 incubation period, it is probable that some incubations turned anoxic when  $\text{CO}_2$  levels exceeded 21%, which occurred primarily  
256 in incubations with glucose or *Mortierella*. This was an unintended consequence of performing the incubations in closed  
257 bottles, which was required to prevent the escape of  $^{13}\text{C}$ -labeled inorganic C. Nevertheless, such alteration between oxic and



258 anoxic conditions is common in natural environments, and the measured inorganic C assimilation into fungal lipids was  
259 consistently low (<3%; Fig. 2), regardless the implied anoxia.  
260



261 **Figure 4. Carbon use efficiency of fungal species from three phyla growing on monomers or complex substrates. Lines**  
262 **were calculated assuming that fungal biomass was 44% C (w/w). Colors and symbols are redundant with Fig. 1.**

263

#### 264 4.2 Fungal IC assimilation into lipids

265 A fundamental process in nature and basis for ecological food webs is the fixation of inorganic C via photosynthesis and  
266 chemosynthesis by autotrophic organisms. Inorganic C assimilation by heterotrophic organisms also plays an important role  
267 in ensuring the provision of energy and to replenish intermediates in the TCA cycle that have been released for biosynthesis  
268 (Kornberg 1965). Therefore, inorganic C assimilation is a measure of both anabolic processes and the catabolic status of the  
269 cell, influenced by assimilation, biosynthesis, anaplerotic reactions and redox balancing reactions (Braun et al., 2021; Erb  
270 2011). Previous reports on the by-fixation of inorganic C (%IC) via anaplerotic pathways into heterotrophic biomass varied  
271 between 1 - 8% (Dijkhuizen & Harder, 1985; Feisthauer et al., 2008; Romanenko 1964; Roslev et al., 2004), whereas for fungi  
272 it was previously reported to amount to roughly 1% (Sorokin 1961; Schinner & Concini, 1981; Schinner et al., 1982), and was  
273 recently shown to vary between 2 – 12% for Ascomycetes when grown on glucose or glutamic acid (Jabinski et al., 2024). Our  
274 results demonstrate a low range in %IC for all different substrates and species tested in this study (0 - 3%), with the  
275 Ascomycetes (0 - 2%) assimilating relatively less inorganic C than previously reported species ( $4.6\% \pm 1.6\%$ ; Jabinski et al.,  
276 2024). The highest incorporation was 2.8% by *Penicillium jancewskii* (PJ) when grown on tannic acid (Table 1; Fig. 3);



277 notably, this experiment yielded high production of CO<sub>2</sub> and biomass, suggesting that increased assimilation of inorganic C  
278 may promote the ability to respire the complex substrate. The high CO<sub>2</sub> levels also suggest that the incubations of PJ with  
279 tannic acid may have turned anoxic, which may also explain the higher inorganic C incorporation in these incubations.

### 280 4.3 Water hydrogen derived Lipid synthesis

281 As demonstrated previously, the regression slope between hydrogen isotopic composition of water medium and microbial  
282 lipids (i.e.,  $\alpha_w$ ) varies with the type of metabolism (Zhang et al., 2009; Valentine, 2009; Wijker et al., 2019; Jabinski et al.,  
283 2024). For fatty acid biosynthesis, H incorporation is suggested to be a function of transporters and electron acceptors (NADPH  
284 and NADH), with contributions accounting for around half of all lipid hydrogen. The remaining comprises equal contributions  
285 of H obtained directly from environmental water or acetyl-CoA (Valentine, 2009; Zhang et al., 2009; Caro et al., 2023). The  
286 consensus from previous studies that investigated the lipids of heterotrophic bacteria is that microbial heterotrophs exhibit  $\alpha_w$   
287 values ranging from 0 to 1.2, with a mean of  $0.71 \pm 0.17$  (e.g., Caro et al., 2023). Jabinski et al. (2024) demonstrated that five  
288 species of heterotrophic Ascomycetes exhibit similar  $\alpha_w$  values ( $0.62 \pm 0.04$ ) for the fungal biomarker C<sub>18:2</sub> during growth on  
289 glucose. In the current study,  $\alpha_w$  values for the fungal biomarker C<sub>18:2</sub> during growth on glucose ( $0.60 \pm 0.05$ ) were agreeable  
290 with Jabinski et al. (2024), but more variable, likely owing to the broader phylogenetic coverage of the current study. However,  
291 significant differences in  $\alpha_w$  values were observed both between and within the different phyla and substrates tested.  
292 Ascomycetes species exhibited the most consistent  $\alpha_w$  values when grown on each of the four different substrates [ $0.63 \pm 0.03$   
293 (Glu);  $0.78 \pm 0.01$  (SA);  $0.76 \pm 0.02$  (TA);  $0.67 \pm 0.01$  (BC)]. Basidiomycetes only produced enough biomass for isotopic  
294 analysis when grown on glucose and  $\beta$ -cyclodextrin, and showed high variability in  $\alpha_w$  between species. For example, during  
295 growth on glucose, *P. involutus* exhibited much higher  $\alpha_w$  values than *P. chrysosporium* ( $0.75 \pm 0.06$  versus  $0.37 \pm 0.03$ ,  
296 respectively), and both of these values were beyond the more confined range of  $\alpha_w$  values determined for Zygomycetes and  
297 Ascomycetes species. Growth on  $\beta$ -cyclodextrin, which consists of seven glucanopyranose units (C<sub>6</sub>H<sub>12</sub>O<sub>6</sub>), exhibited similar  
298  $\alpha_w$  values ( $0.58 \pm 0.06$ ) as growth on glucose ( $0.60 \pm 0.05$ ), suggesting that the catabolism of glucose subunits via glycolysis  
299 overprints signals of water-H incorporation that may derive during degradation of  $\beta$ -cyclodextrin. Succinate yielded  
300 significantly higher  $\alpha_w$  values ( $0.83 \pm 0.05$ ), which was more similar to that reported previously for glutamic acid ( $0.90 \pm 0.07$ ;  
301 Jabinski et al., 2024). A one-way analysis of variance (ANOVA; Holm-Sidak method; SigmaPlot v11) confirmed the  
302 significant difference between glucose and glutamic acid ( $p < 0.001$ ), glutamic acid and  $\beta$ -cyclodextrin ( $p < 0.001$ ), succinate  
303 and glucose ( $p < 0.003$ ) and succinate and  $\beta$ -cyclodextrin ( $p < 0.005$ ). It also confirmed that there was no significant difference  
304 between the other substrate combinations ( $p > 0.005$ ). Notably, glutamic acid and succinate are thought to be introduced into  
305 the TCA cycle through coupled metabolites, where succinate is a direct metabolite inside the TCA cycle and glutamic acid is  
306 converted to  $\alpha$ -ketoglutarate intermediate by transamination before entering the TCA cycle, which is only 2 steps from  
307 succinate (Cooper et al., 2014). Also, being acids, these substrates may have a greater capacity than saccharides to exchange  
308 H with ambient water at experimental pH (typically  $2 < \text{pH} < 5.2$ ), especially glutamic acid, which also comprises an amino  
309 moiety. Tannic acid ( $0.76 \pm 0.02$ ) yielded no significant differences ( $p > 0.005$ ) from the other substrates, and is reported to



310 be degraded to different subunits including gallic acid and glucose (Banerjee and Mahapatra, 2012; Lekha and Lonsane, 1997  
311 and references within). Aromatic degradation pathways employed by fungi generate intermediates that go through the  $\beta$ -  
312 keto adipate pathway (Mäkelä et al., 2015) before entering the TCA cycle as a succinyl-CoA metabolite (Lekha and Lonsane,  
313 1997). The  $\alpha_w$  values induced by degradation of TA suggest that it integrates both the low  $\alpha_w$  signature of glycolysis and high  
314  $\alpha_w$  signature of the TCA cycle (Fig. 5).

315 Together, our incubation experiments suggest that  $\alpha_w$  values determined for the fungal biomarker  $C_{18:2}$  could not distinguish  
316 between fungal growth on relatively labile monomers (i.e., glucose and succinate; requiring as few as 5 days of cultivation)  
317 versus larger, less-labile substrates (i.e.,  $\beta$ -cyclodextrin and tannic acid; requiring 20 to 183 days of cultivation). However,  
318 with the exception of Basidiomycetes,  $\alpha_w$  values of fungal lipid biomarkers may be indicative of fungi employing primarily  
319 glycolytic or TCA pathways. Environmental assays that quantify fungal lipid production via the incorporation of ambient  
320 water-H (i.e., the lipid-SIP approach) may upscale to total production estimates by applying our calculated mean  $\alpha_w$  value of  
321  $0.69 \pm 0.03$  [ $n = 27$ ;  $\pm$  (SEM)], which is consistent with the  $\alpha_w$  value of 0.71 recommended for soil microbial communities  
322 (Caro et al., 2023).

#### 323 4.4 Dual-SIP approach

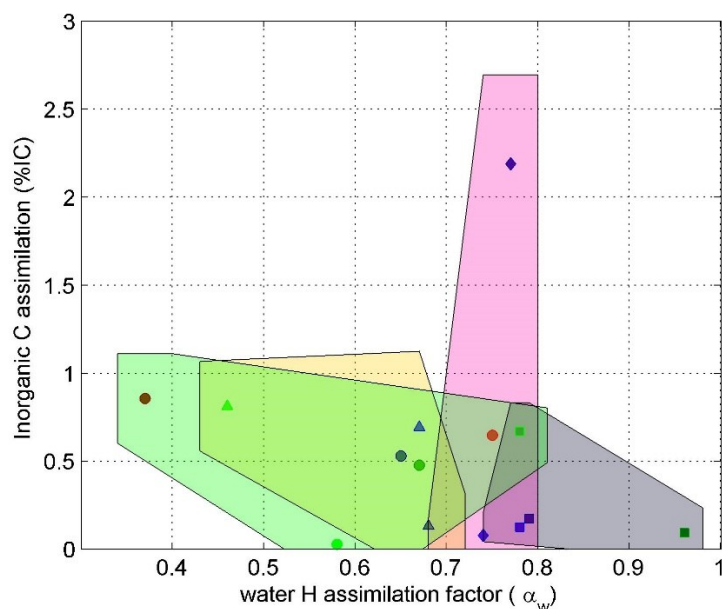
324 Dual-SIP experiments with  $^2H_2O$  and  $^{13}C$ -dissolved IC previously highlighted the potential to track microbial activity and  
325 distinguish heterotrophic vs autotrophic metabolic modes within environmental settings and pure cultures (Kellerman et al.,  
326 2012, 2016; Wegener et al., 2012; Huguet et al., 2017; Wu et al., 2018, 2020). This approach was also previously applied to  
327 investigate fungal pure cultures (Jabinski et al., 2024), in which the plot of assimilation of inorganic C versus water-H into the  
328 fungal biomarker  $C_{18:2}$  could distinguish five Ascomycetes species growing on glucose or glutamic acid, with  $\alpha_w$  values  
329 explaining most of the variability. While calculated IC: $\alpha_w$  are useful to distinguish autotrophic from heterotrophic growth, all  
330 calculated values in this study remained near zero, with %IC ranging up to 3% and  $\alpha_w$  values ranging from 0.6 to 0.8. This  
331 pure culture study therefore suggests that fungal assimilation of inorganic C is low and less insightful than the more  
332 distinguishable  $\alpha_w$  values for identifying fungal phylotypes or ecotypes in environmental assays.

#### 333 5 Conclusion

334 The purpose of this work was to apply the dual-SIP assay on pure fungal cultures to define the effect of different carbon  
335 substrates on incorporation of water-H and inorganic C into their membrane lipids. Although heterotrophic C fixation by  
336 microbes may range up to 8% of biomass C, inorganic C assimilation into the fungal biomarker  $C_{18:2}$  harvested from six species  
337 representing Ascomycetes, Basidiomycetes, and Zygomycetes did not vary consistently between species or substrate, and  
338 remained below 3%. However, *Penicillium jancewskii*, the species that was most successful at respiring tannic acid, also  
339 exhibited the highest %IC value of all incubations (Fig. 1; Fig. 5), suggesting that fungal degradation of similarly complex  
340 substrates may rely in part on the assimilation of inorganic C (e.g., via anaerobic reactions).



341



342

343 **Figure 5. %IC and  $\alpha_w$  value scatter plot for  $C_{18:2}$  identifying the grouping of glucose (circles, green shape), succinic acid (squares,**  
344 **grey shape), tannic acid (diamonds, pink shape) and  $\beta$ -cyclodextrin (triangles, yellow shape) incubations with Ascomycetes,**  
345 **Basidiomycetes, and Zygomycetes. Refer to Fig. 1. Caption for further details.**

346 In contrast to %IC, we conclude that substrates that activated the glycolysis pathway yielded significantly lower  $\alpha_w$  values  
347 than those catabolized as TCA intermediates. The expanded dataset provided by this study indicates that inorganic C  
348 assimilation by heterotrophic fungi accounts for < 3% of lipid carbon, and fungal production estimated by  $^2\text{H}$ -lipid SIP  
349 experiments can be adjusted by an average  $\alpha_w$  value of 0.69, to provide a more accurate estimate of total lipid production.  
350 Furthermore, determination of  $\alpha_w$  values in environmental  $^2\text{H}$ -SIP assays may be useful to identify the prevalence of fungal  
351 ecotypes that rely on C substrates fueling glycolysis (e.g., leaf litter) versus those that are fed primarily by TCA intermediates  
352 (e.g., root exudate).

353

#### 354 **Data availability**

355 Data presented in the figures and tables can be obtained by contacting the corresponding author and will be made available on  
356 the Fractome Database (<https://fractome.caltech.edu/>).

357

#### 358 **Author contribution**

359 Stanislav Jabinski, Conceptualization, Data curation, Formal analysis, Investigation, Methodology, Software, Validation,  
360 Visualization, Writing – original draft, Writing – review and editing

361 Vítězslav Kučera, Investigation, Methodology, Resources, Writing – review and editing



362 Marek Kopáček, Formal analysis, Methodology, Resources, Validation,  
363 Jan Jansa, Conceptualization, Formal analysis, Methodology, Resources, Validation, Writing – review and editing  
364 Travis B. Meador, Conceptualization, Data curation, Formal analysis, Funding acquisition, Investigation, Methodology,  
365 Project administration, Resources, Software, Supervision, Validation, Visualization, Writing – original draft, Writing – review  
366 and editing

### 367 **Competing interests**

368 The authors declare that they have no conflict of interest.

### 369 **Disclaimer**

### 370 **Acknowledgements**

371 We thank Ljubov Polaková for the support of the stable isotope measurements and laboratory protocols; the Collection of  
372 Microscopic Fungi of the Institute of Soil Biology BC CAS for providing the fungal species *Penicillium janczewskii* strain  
373 BCCO20\_0265 and the Institute of Microbiology CAS for providing the fungal species *Paxillus involutus* strain  
374 SB-22; *Phanerochaete chrysosporium* strain CCM8074, *Mortierella* strain RK-38; *Umbelopsis* strain RK-43 and *Paecilomyces*  
375 *lilacinus* strain DP-23.

376 This Project was funded by the Czech Science Foundation GACR nr. 20-223805 (FUNSIF) and supported by MEYS CZ grant  
377 LM2015075 Projects of Large Infrastructure for Research, Development and Innovations as well as the European Regional  
378 Development Fund-Project: research of key soil-water ecosystem interactions at the SoWa Research Infrastructure (No.  
379 CZ.02.1.01/0.0/0.0/16\_013/0001782).

380

### 381 **References**

382 Baldrian, P., Voříšková, J., Dobiášová, P., Merhautová, V., Lisá, L., & Valášková, V. (2011). Production of extracellular  
383 enzymes and degradation of biopolymers by saprotrophic microfungi from the upper layers of forest soil. *Plant and Soil*,  
384 338(1-2), 111-125. doi:10.1007/s11104-010-0324-3

385 Banerjee, D., & Mahapatra, S. (2012). Fungal tannase: a journey from strain isolation to enzyme applications. *Dyn Biochem*  
386 *Process Biotechnol Mol Biol*, 6(2), 49-60.

387 Boer, W. D., Folman, L. B., Summerbell, R. C., & Boddy, L. (2005). Living in a fungal world: impact of fungi on soil bacterial  
388 niche development. *FEMS microbiology reviews*, 29(4), 795-811.

389 Boschker HTS, Middelburg JJ. 2002. Stable isotopes and biomarkers in microbial ecology. *FEMS Microbiol Ecol* 40:85–95.  
390 <https://doi.org/10.1111/j.1574-6941.2002.tb00940.x>

391 Boschker, H. T. S., Nold, S. C., Wellsbury, P., Bos, D., De Graaf, W., Pel, R., ... & Cappenberg, T. E. (1998). Direct linking  
392 of microbial populations to specific biogeochemical processes by <sup>13</sup>C-labelling of biomarkers. *Nature*, 392(6678), 801-805.





- 393 Braun A, Spona-Friedl M, Avramov M, Elsner M, Baltar F, Reinthaler T, Herndl GJ, Griebler C. 2021. Reviews and syntheses:  
394 heterotrophic fixation of inorganic carbon—significant but invisible flux in environmental carbon cycling. *Biogeosciences*  
395 18:3689–3700. <https://doi.org/10.5194/bg-18-3689-2021>
- 396 Bukovská P, Bonkowski M, Konvalinková T, Beskid O, Hujšlová M, Püschel D, et al. Utilization of organic nitrogen by  
397 arbuscular mycorrhizal fungi—is there a specific role for protists and ammonia oxidizers? *Mycorrhiza*. 2018;28(3):269–83.  
398 <https://doi.org/10.1007/s00572-018-0825-0>.
- 399 Carlson C.A., N.R. Bates, D.A. Hansell, D.K. Steinberg. 2001. Carbon Cycle. In: J. Steele, S. Thorpe, K. Turekian (Eds.)  
400 Encyclopedia of Ocean Science, 2nd Edition. Academic Press, 477-486.
- 401 Caro, T. A., McFarlin, J., Jech, S., Fierer, N., & Kopf, S. (2023). Hydrogen stable isotope probing of lipids demonstrates slow  
402 rates of microbial growth in soil. *Proceedings of the National Academy of Sciences*, 120(16), e2211625120.
- 403 Ciais, P., Dolman, A. J., Bombelli, A., Duren, R., Pregon, A., Rayner, P. J., . . . Marland, G. (2014). Current systematic  
404 carbon-cycle observations and the need for implementing a policy-relevant carbon observing system. *Biogeosciences*, 11(13),  
405 3547-3602. doi:10.5194/bg-11-3547-2014
- 406 Cooper AJL, Kuhara T. 2014.  $\alpha$ -Ketoglutaramate: an overlooked metabolite of glutamine and a biomarker for hepatic  
407 encephalopathy and inborn errors of the urea cycle. *Metab Brain Dis* 29:991–1006. [https://doi.org/10.1007/s11011-013-9444-](https://doi.org/10.1007/s11011-013-9444-9)  
408 9
- 409 Dijkhuizen, L., & Harder, W. (1985). Microbial metabolism of carbon dioxide. *Comprehensive biotechnology: the principles,*  
410 *applications, and regulations of biotechnology in industry, agriculture, and medicine*/editor-in-chief, Murray Moo-Young.
- 411 Dumont, M. G., & Murrell, J. C. (2005). Stable isotope probing—linking microbial identity to function. *Nature Reviews*  
412 *Microbiology*, 3(6), 499-504.
- 413 Erb TJ. 2011. Carboxylases in natural and synthetic microbial pathways. *Appl Environ Microbiol* 77:8466–8477.  
414 <https://doi.org/10.1128/AEM.05702-11>
- 415 Feisthauer, S., Wick, L. Y., Kästner, M., Kaschabek, S. R., Schlömann, M., & Richnow, H. H. (2008). Differences of  
416 heterotrophic  $^{13}\text{C}$  assimilation by *Pseudomonas knackmussii* strain B13 and *Rhodococcus opacus* 1CP and potential impact  
417 on biomarker stable isotope probing. *Environmental Microbiology*, 10(6), 1641-1651.
- 418 Fioretto, A., Di Nardo, C., Papa, S., & Fuggi, A. (2005). Lignin and cellulose degradation and nitrogen dynamics during  
419 decomposition of three leaf litter species in a Mediterranean ecosystem. *Soil Biology and Biochemistry*, 37(6), 1083-1091.  
420 doi:10.1016/j.soilbio.2004.11.007
- 421 Fischer, C. R., Bowen, B. P., Pan, C., Northen, T. R., & Banfield, J. F. (2013). Stable-isotope probing reveals that hydrogen  
422 isotope fractionation in proteins and lipids in a microbial community are different and species-specific. *ACS chemical biology*,  
423 8(8), 1755-1763.
- 424 Frey, S. D. (2019). Mycorrhizal fungi as mediators of soil organic matter dynamics. *Annual review of ecology, evolution, and*  
425 *systematics*, 50, 237-259. doi:10.1146/annurev-ecolsys-110617-062331



- 426 Grinhut, T., Hadar, Y., & Chen, Y. (2007). Degradation and transformation of humic substances by saprotrophic fungi:  
427 processes and mechanisms. *Fungal biology reviews*, 21(4), 179-189.
- 428 Hoefs, J. (2018). *Stable isotope geochemistry*. Springer International Publishing AG, part of Springer Nature. doi:10.1007/978-  
429 3-319-78527-1
- 430 HoÈgberg, P., Nordgren, A., Buchmann, N., Taylor, A. F., Ekblad, A., HoÈgberg, M. N., . . . Read, D. J. (2001). Large-scale  
431 forest girdling shows that current photosynthesis drives soil respiration. *Nature*, 411(6839), 789-792.
- 432 Huguet, A., Meador, T. B., Laggoun-Défarge, F., Könnenke, M., Wu, W., Derenne, S., & Hinrichs, K.-U. (2017). Production  
433 rates of bacterial tetraether lipids and fatty acids in peatland under varying oxygen concentrations. *Geochimica et*  
434 *Cosmochimica Acta*, 203, 103-116. doi:10.1016/j.gca.2017.01.012
- 435 Jabinski, S., d. M. Rangel, W., Kopáček, M., Jílková, V., Jansa, J., & Meador, T. B. (2024). Constraining activity and growth  
436 substrate of fungal decomposers via assimilation patterns of inorganic carbon and water into lipid biomarkers. *Applied and*  
437 *Environmental Microbiology*, 90(4), e02065-23.
- 438 Kellermann, M. Y., Wegener, G., Elvert, M., Yoshinaga, M. Y., Lin, Y.-S., Holler, T., . . . Hinrichs, K.-U. (2012). Autotrophy  
439 as a predominant mode of carbon fixation in anaerobic methane-oxidizing microbial communities. *Proceedings of the National*  
440 *Academy of Sciences*, 109(47), 19321-19326. doi:10.1073/pnas.1208795109
- 441 Kellermann, M. Y., Yoshinaga, M. Y., Wegener, G., Krukenberg, V., & Hinrichs, K.-U. (2016). Tracing the production and  
442 fate of individual archaeal intact polar lipids using stable isotope probing. *Organic Geochemistry*, 95, 13-20.  
443 doi:10.1016/j.orggeochem.2016.02.004
- 444 Kirk, T. K., & Farrell, R. L. (1987). Enzymatic" combustion": the microbial degradation of lignin. *Annual Reviews in*  
445 *Microbiology*, 41(1), 465-501. doi:10.1146/annurev.mi.41.100187.002341
- 446 Kopf, S. H., McGlynn, S. E., Green-Saxena, A., Guan, Y., Newman, D. K., & Orphan, V. J. (2015). Heavy water and (15) N  
447 labelling with NanoSIMS analysis reveals growth rate-dependent metabolic heterogeneity in chemostats. *Environ Microbiol*,  
448 17(7), 2542-2556. doi:10.1111/1462-2920.12752
- 449 Kornberg HL. 1965. Anaplerotic sequences in microbial metabolism. *Angew Chem Int Ed Engl* 4:558–565.  
450 <https://doi.org/10.1002/anie.196505581>
- 451 Kreuzer-Martin, H. W. (2007). Stable isotope probing: linking functional activity to specific members of microbial  
452 communities. *Soil Science Society of America Journal*, 71(2), 611-619.
- 453 Lekha, P. K., & Lonsane, B. K. (1997). Production and application of tannin acyl hydrolase: state of the art. *Advances in*  
454 *applied microbiology*, 44, 215-260.
- 455 Lindahl, B. D., & Tunlid, A. (2015). Ectomycorrhizal fungi–potential organic matter decomposers, yet not saprotrophs. *New*  
456 *Phytologist*, 205(4), 1443-1447. doi:10.1111/nph.13201
- 457 Osburn, M. R., Sessions, A. L., Pepe-Ranney, C., & Spear, J. R. (2011). Hydrogen-isotopic variability in fatty acids from  
458 Yellowstone National Park hot spring microbial communities. *Geochimica et Cosmochimica Acta*, 75(17), 4830-4845.
- 459 Romanenko VI. 1964. Heterotrophic assimilation of CO<sub>2</sub> by bacterial flora of water. *Mikrobiologija* 33:679–683.



- 460 Roslev P, Larsen MB, Jørgensen D, Hesselsoe M. 2004. Use of heterotrophic CO<sub>2</sub> assimilation as a measure of metabolic  
461 activity in planktonic and sessile bacteria. *J Microbiol Methods* 59:381–393. <https://doi.org/10.1016/j.mimet.2004.08.002>
- 462 Sachse, D., Billault, I., Bowen, G. J., Chikaraishi, Y., Dawson, T. E., Feakins, S. J., ... & Kahmen, A. (2012). Molecular  
463 paleohydrology: interpreting the hydrogen-isotopic composition of lipid biomarkers from photosynthesizing organisms.  
464 *Annual Review of Earth and Planetary Sciences*, 40, 221-249.
- 465 Schinner F, Concini R, Binder H. 1982. Heterotrophic CO<sub>2</sub> fixation by fungi in dependence on the concentration of the carbon  
466 source. Paper presented at the Phytos; *annales rei botanicae*
- 467 Schinner F, Concini R. 1981. Carbon dioxide fixation by wood-rotting fungi. *Eur J For Pathol* 11:120–123.  
468 <https://doi.org/10.1111/j.1439-0329.1981.tb00077.x>
- 469 Smith, S. E., & Read, D. (2008). Mineral nutrition, toxic element accumulation and water relations of arbuscular mycorrhizal  
470 plants. *Mycorrhizal symbiosis*, 3, 145-148. doi:10.1016/B978-012370526-6.50007-6
- 471 Šnajdr, J., Cajthaml, T., Valášková, V., Merhautová, V., Petránková, M., Spetz, P., . . . Baldrian, P. (2011). Transformation of  
472 *Quercus petraea* litter: successive changes in litter chemistry are reflected in differential enzyme activity and changes in the  
473 microbial community composition. *FEMS Microbiology Ecology*, 75(2), 291-303. doi:10.1111/j.1574-6941.2010.00999.x
- 474 Sorokin, J. I. (1966). On the carbon dioxide uptake during the cell synthesis by microorganisms. *Zeitschrift für allgemeine*  
475 *Mikrobiologie*, 6(1), 69-73. doi:10.1002/jobm.3630060107
- 476 Sorokin, Y. I. (1961). Heterotrophic carbon dioxide assimilation by microorganisms. *Zhurnal Obshchei Biologii*, 22(4), 265-  
477 272.
- 478 Treonis, A. M., Ostle, N. J., Stott, A. W., Primrose, R., Grayston, S. J., & Ineson, P. (2004). Identification of groups of  
479 metabolically-active rhizosphere microorganisms by stable isotope probing of PLFAs. *Soil Biology and Biochemistry*, 36(3),  
480 533-537.
- 481 Valentine, D. L. (2009). Isotopic remembrance of metabolism past. *Proceedings of the National Academy of Sciences*, 106(31),  
482 12565-12566. doi:10.1073/pnas.0906428106
- 483 Wegener, G., Bausch, M., Holler, T., Thang, N. M., Prieto Mollar, X., Kellermann, M. Y., . . . Boetius, A. (2012). Assessing  
484 sub-seafloor microbial activity by combined stable isotope probing with deuterated water and <sup>13</sup>C-bicarbonate. *Environmental*  
485 *Microbiology*, 14(6), 1517-1527. doi:10.1111/j.1462-2920.2012.02739.x
- 486 Wegener, G., Kellermann, M. Y., & Elvert, M. (2016). Tracking activity and function of microorganisms by stable isotope  
487 probing of membrane lipids. *Current Opinion in Biotechnology*, 41, 43-52. doi:10.1016/j.copbio.2016.04.022
- 488 Wijker, R. S., Sessions, A. L., Fuhrer, T., & Phan, M. (2019). 2H/1H variation in microbial lipids is controlled by NADPH  
489 metabolism. *Proceedings of the National Academy of Sciences*, 116(25), 12173-12182. doi:10.1073/pnas.1818372116
- 490 Willers, C., Jansen van Rensburg, P. J., & Claassens, S. (2015). Phospholipid fatty acid profiling of microbial communities—a  
491 review of interpretations and recent applications. *Journal of applied microbiology*, 119(5), 1207-1218.
- 492 Wu W, Meador T, Hinrichs K-U. 2018. Production and turnover of microbial organic matter in surface intertidal sediments.  
493 *Org Geochem* 121:104–113. <https://doi.org/10.1016/j.orggeochem.2018.04.006>



494 Wu, W., Meador, T. B., Könneke, M., Elvert, M., Wegener, G., & Hinrichs, K. U. (2020). Substrate-dependent incorporation  
495 of carbon and hydrogen for lipid biosynthesis by *Methanosarcina barkeri*. *Environmental Microbiology Reports*, 12(5), 555-  
496 567. doi:10.1111/1758-2229.12876  
497 Zhang, X., Gillespie, A. L., & Sessions, A. L. (2009). Large D/H variations in bacterial lipids reflect central metabolic  
498 pathways. *Proceedings of the National Academy of Sciences*, 106(31), 12580-12586. doi:10.1073/pnas.0903030106  
499  
500